Proceedings of the 1st Global Power and Propulsion Forum
GPPF 2017
Jan 16-18, 2014, Zurich, Switzerland
www.pps.global

GPPF-2017-36

OPTIMUM PROPULSION CYCLES FOR UNMIXED AND MIXED TURBOFANS

Adel Ghenaiet
Laboratory of Energetics and Conversion Systems, Faculty of Mechanical Engineering, University of Sciences and Technology, USTHB, BP32 El-Alia, Bab-ezzouar, 16111, Algiers,
ag1964@yahoo.com
Algeria

ABSTRACT

The optimization of aero-engines in early stages is necessary to reduce the development cost and time. This paper presents the results of the parametric study and the optimization of the design parameters for unmixed and mixed high bypass turbofans. The based simulation programs do not use the engine components' maps, which are not usually available, but rely on aerothermodynamic models. The parametric analysis concentrated on studying the effects of the principal design parameters (turbine entry temperature, high-pressure ratio, low-pressure, fan pressure ratio and bypass ratio) on the propulsive performance and the feasible design space. The optimization based on a genetic algorithm consisted in finding the optimum propulsion cycles for unmixed and mixed turbofans minimizing the specific fuel consumption and satisfying the thrust in cruise and takeoff for a long-range airliner, as well as technology constraints and pollutant emissions. The cruise flight conditions critical for fuel burn is a key characteristic in selecting the appropriate cycle configuration.

INTRODUCTION

Aero-engines powering advanced long range and large capacity airliners are targeting higher thrust at takeoff and lower fuel consumption, pollutants and noise. Indeed, there was about 50% improvement [1] in the specific fuel consumption TSFC when engines evolved from the early turbojets to the high bypass turbofans of modern time. In addition, the specific thrust reduced significantly [2] as the bypass ratio (BPR) increased up to 10. The prediction of an engine performance is very useful in preliminary design sizing and matching to airframes [3], starting from the request of proposal defining all the specifications and requirements. Engines simulation programs used in predicting the performance of propulsion systems are valuable tools in preliminary sizing. Today many computerized tools are at the design engineer's disposal for considering the components and engine design characteristics, for example: GasTurb [4], GSP [5], NPSS [6], which require the components performance maps. Kurzke [7] with the help of a gradient-based optimization algorithm coupled to a component-level code GasTurb conducted an optimization task to adapt an existing engine to a new application. Sanghi et al. [8] elaborated a procedure to search for the design point of an engine, targeting minimum fuel consumed during a prescribed flight mission. Sane et al. [9] utilized the response surface surrogate optimizer for the optimum design of a high-bypass turbofan. The paper presented by Jorge de Luis and Mavris [10] summarizes the steps of sizing a turbofan with separate nozzles for a specified flight condition. The minimization of TSFC consists in finding the optimum pressure ratios for the fan and the low-pressure turbine found for any flight altitude and Mach number combination, depending on the characteristics of the cycle and the components efficiencies. Yadav et al. [11] presented a detailed parametric analysis of all the possible configurations of turbofan engine (two and three spool with or without mixer). The prediction of engine dependent parameters (i.e. specific thrust, TSFC, propulsive efficiency, efficiency of energy conversion and overall efficiency) at varying independent parameters was possible at any flight condition and for any set of operating parameters. Rybakov et al. [12] described the method of optimization of engine core parameters jointly with optimization of values of every engine forming the line of engines developed on the basis of this core. Syed Khalid [13] presented studies of both mixed and separate exhaust turbofans with design BPR toward predicting the improvement for the whole engine system. Comparison between mixed exhaust and separate exhaust configurations with the same BPR showed advantage with mixed exhaust designs up to a design BPR of 7. However, for a design BPR of 8 the mixed exhaust design showed worse TSFC than the separate exhaust turbofan. In addition, a comparison of gross

thrust at the off-design condition revealed a gain of mixed exhaust design up to a design BPR of 7, and a loss in thrust for a design BPR of 8.

The present paper examines thoroughly the effects of propulsion cycle parameters on the propulsive performance of both mixed and unmixed turbofan engines. The search of best configuration within the delimited feasible design space resulted in the optimum parameters, considering the power requirements and constraints related to the technology level and operating conditions. The thrust requirement in cruise and takeoff were previously assessed [14] for a model of long-range airliner.

PARAMETRIC STUDY AND ANALYSIS

Figure 1 depicts the two configurations of turbofan engines. The fundamental parameters are the temperature inlet temperature (TIT), overall pressure ratio (OPR) (product of low-pressure ratio (LPR) and high-pressure ratio (HPR)), fan pressure ratio (FPR) and BPR. Typical values of components efficiencies are compiled from several references [15], [16]. Power extraction used the same as the reference engine CF6-80A3 [17]. The fractions of air-cooling used for NGVs and rotor blades are estimated by a fit for the graphical relations published by Walsh and Fletcher [18].

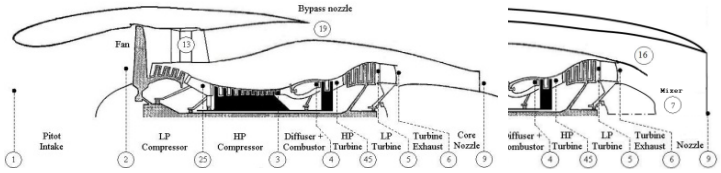

Figure 1: Unmixed mixed turbofan layout and stations numbering

The mass flow rates through the bypass duct, different compressors and turbines stages and nozzles are related to the total intake air mass flow rate, fuel fraction and air-cooling and air-bleed fractions. The flow properties at any component station used compressible flow functions and enthalpies of air and gas mixtures. By considering the burner efficiency correlated against the combustor loading factor and energy balance across the combustor, yields an estimate of the local and the overall fuel by air ratio for the used fuel type Jet A.

$$\mathrm{f} = \frac{h_{tg}(T_{t4}, f) - h_{t3}(T_{t3})}{\eta_b Lcv - h_{tg}(T_{t4}, f)} \quad , \quad \tau_b = \frac{Cp_4}{Cp_0}\frac{T_{t4}}{T_0} \tag{1}$$

The equilibrium running of HP spool yields the expansion parameters for HP turbine:

$$\tau_{TH} = 1 - \frac{\overline{Cp}_{25-3} C_{g4}}{\eta_{mH} \overline{Cp}_{4-45} Cp_0}\left[\frac{\tau_r \tau_{CL}(\tau_{CH} - 1)}{\tau_b(1+f)(1-\beta-\varepsilon_{TH}-\varepsilon_{TL}) + \varepsilon_{TH}\tau_r\tau_{CL}\tau_{CH}}\right] \tag{2a}$$

$$\pi_{TH} = \tau_{TH}^{\frac{\gamma_4}{e_{TH}(\gamma_4 - 1)}} \tag{2b}$$

Similarly the expansion parameters for LP turbine:

$$\tau_{TL} = 1 - \frac{Cp_4}{Cp_0}\frac{\tau_r}{\eta_{mL}\tau_{TH}}\left[\frac{\frac{\overline{Cp}_{2-25}}{\overline{Cp}_{45-5}}(\tau_{CL} - 1) + \frac{\overline{Cp}_{2-13}}{\overline{Cp}_{45-5}}\alpha(\tau_F - 1) + (1+\alpha)C_{TO}/\eta_{ml}}{(1+f)(1-\beta-\varepsilon_{TH}-\varepsilon_{TL})\tau_b + (\varepsilon_{TH} + \varepsilon_{TL}/\tau_{TH})\tau_r\tau_{CL}\tau_{CH}}\right] \tag{3a}$$

$$C_{TOi} = Power_{ext}/Cp_{a0}T_0 m_0 \quad , \quad \pi_{TL} = \tau_{TL}^{\frac{\gamma_{45}}{e_{TL}(\gamma_{45}-1)}} \tag{3b}$$

For an unmixed turbofan, the total thrust is the summation of the core stream thrust and the bypass stream thrust:

$$F_c = \dot{m}_9(V_9 - V_0) + A_9(P_9 - P_0) \tag{4a}$$

$$F_F = \dot{m}_F(V_{19} - V_0) + A_{19}(P_{19} - P_0) \tag{4b}$$

TSFC is based the overall specific thrust and fuel ratio:

$$TSFC = f_0(F/\dot{m}_0)^{-1} \tag{4c}$$

$$f_o = f(1 - \beta - \varepsilon_{TH} - \varepsilon_{TL})/(1+\alpha) \tag{4d}$$

The specific thrust is the ratio between the thrust and the intake air mass flow rate. The separate specific thrusts of the core and bypass as given bellow involve the static temperature, pressure and velocity ratio:

$$\frac{F_c}{\dot{m}_0} = \frac{a_0}{\alpha+1}\left[(1+f_o-\beta)\frac{V_9}{a_0} - M_0 + (1+f_o-\beta)\frac{R_{g9}}{\gamma_{a0}R_{a0}}\frac{T_9/T_0}{V_9/a_0}\left(1 - \frac{P_0}{P_9}\right)\right] \tag{5a}$$

$$\frac{F_F}{\dot{m}_0} = a_0\frac{\alpha}{\alpha+1}\left[\frac{V_{19}}{a_0} - M_0 + \frac{R_{g19}}{\gamma_{a0}R_{a0}}\frac{T_{19}/T_0}{V_{19}/a_0}\left(1 - \frac{P_0}{P_{19}}\right)\right] \tag{5b}$$

Where the overall ratios of temperature, pressure and velocity:

$$\frac{P_0}{P_9} = \left[\pi_r\pi_d\pi_{CL}\pi_{CH}\pi_b\pi_{TH}\pi_{TL}\pi_N\right]^{-1}\frac{P_{t9}}{P_9} \tag{6a}$$

$$\frac{T_9}{T_0} = \frac{Cp_{a0}}{Cp_{g9}}\tau_b\tau_{mth}\tau_{TH}\tau_{mtl}\tau_{TL}\Big/\frac{T_{t9}}{T_9} \tag{6b}$$

$$\frac{V_9}{a_0} = M_9\sqrt{\frac{R_9}{R_0}\frac{\gamma_9}{\gamma_0}\left(\frac{T_9}{T_0}\right)} \tag{6c}$$

$$\frac{P_0}{P_{19}} = \left[\pi_r\pi_d\pi_F\pi_{FN}\right]^{-1}\frac{P_{t19}}{P_{19}} \tag{6d}$$

$$\frac{T_{19}}{T_0} = \tau_r\tau_F\Big/\frac{T_{t19}}{T_{19}} \tag{6e}$$

$$\frac{V_{19}}{a_0} = M_{19}\sqrt{\frac{R_{19}}{R_0}\frac{\gamma_{19}}{\gamma_0}\left(\frac{T_{19}}{T_0}\right)} \tag{6f}$$

The expansion parameters of primary nozzle and secondary nozzle depend on choking conditions:

$$\frac{P_{t9}}{P_9} \geq \left(\frac{\gamma_9+1}{2}\right)^{\frac{\gamma_9}{(\gamma_9-1)}} \quad , \quad \frac{P_{t19}}{P_{19}} \geq \left(\frac{\gamma_{19}+1}{2}\right)^{\frac{\gamma_{19}}{(\gamma_{19}-1)}} \tag{7}$$

In the case of a mixed turbofan the thrust and specific thrust are given by equations (4a) and (5a), considering the same overall ratios of temperature, pressure and velocity. The coefficient of enthalpy and total pressure losses due to mixing τ_{mx} and π_{mx} obtained from the conservation equations of mass, energy and momentum. The Mach number M_6 is selected equal to 0.4 and the areas ratio A_{16}/A_6 is estimated within the iterations and found in the same proportion as the reference engine:

$$\tau_{mx} = \frac{Cp_6}{Cp_7}\frac{1 + \alpha(Cp_{16}T_{t16}/Cp_6T_{t6})}{1+\alpha} \tag{8a}$$

$$\pi_{mx} = \pi_m\frac{(1+\alpha)\sqrt{\tau_{mx}}}{1 + A_{16}/A_6}\frac{MFP_6}{MFP_7} \tag{8b}$$

Static pressures P_{16} and P_6 at the inlet of mixer must be set equal, subsequently the convergence becomes difficult to ensure especially in off-design calculations.

Validation

First, the cycle analyzer results for both on-design (cruise flight) and off-design (at takeoff) are compared with those of the reference engines CF6-80A [17] and P&W JT8-D17 [19]. According to Table 1 and Table 2, the predicted results are

quite acceptable despite discrepancies mainly due to the selected values of efficiencies and pressure losses of different components. These discrepancies in term of thrust specific fuel consumption are of order 3.5% and 10%, whereas those in term of thrust are of order 8% and 2%, at design point and off-design conditions, respectively.

Table 1: Validation for the unmixed turbofan

Parameters	Reference engine data [17]		Calculated	
	Takeoff Std+33°F M_0=0, H=0	Cruise Std day M_0=0.8, H=35kft	Takeoff Std+33°F M_0=0 H=0	Cruise Std day M_0=0.8, H=35kft
m_0 (kg/s)	678.5	275.5	678.5	286.04
Thrust (kN)	217.883	48.0407	216.276	48.295
F/m_0(N/kg/s)	321.124	174.37	318.723	168.836
TSFC(mg/Ns)	10.027	17.533	10.646	18.551

Table 2: Validation for the mixed turbofan

Parameters	Reference engine data [19]		Calculated	
	Takeoff day 84°F Static, H=0kft	*Cruise* std+10°C M_0=0.8, H=35kft	*Takeoff* day 84°F Static, H=0kft	*Cruise* std+10°C M_0=0.8, H=35kft
m_0 (kg/s)	145.15	59.42	146.50	56.14
Thrust (N)	71212.5	18815.04	71343.62	17319.41
F/m_0(N/kg/s)	490.61	316.65	486.98	308.50
TSFC(kg/Nh)	0.0625	0.08341	0.064412	0.086375

Parametric Analysis of Unmixed Turbofan

The qualitative results obtained from the preliminary parametric study in cruise flight conditions (Mach=0.8, altitude=35kft, standard day), considering a constant design total inlet air mass flow rate but not including the effect intake installation penalty. High value of BPR is a natural choice for commercial aero-engines because of lower TSFC, but entails higher intake diameter and offset of flow path between the fan and the core, accompanied by an increase in LP turbine stages. The optimum FPR increases with TIT, but on the contrary with increased BPR. The effect of BPR on specific thrust with different FPR and for two values of TIT 1400 K and 1600 K and OPR=35 are depicted in Fig.2. High TIT results in higher specific thrust for all values of BPR, and even more for higher values of FPR. A trade-off is required when selecting the final values of BPR and FPR. As shown by Fig. 3, BPR has a positive effect on TSFC until an optimum that depends on FPR. Subsequently, when operating at high BPR it is interesting to choose a low FPR. The fundamental significance of FPR is its strong impact on the specific thrust and the propulsive efficiency, as depicted by Fig. 4 revealing essentially an increase in the specific thrust with FPR for low values of BPR. On the other hand, large values of BPR intended to reduce TSFC leads to an optimal FPR that tends to drop. The effect on TSFC is also evident from Fig. 5 depicting an optimum of FPR for the given BPR. The minimum of TSFC is located to the left for the large values of BPR, say for example the combination of BPR=10 with FPR=1.45.

Figure 6 plots TSFC versus specific thrust (space of criteria BPR-OPR) for two values of TIT and FPR. The large values of BPR allow using high TIT to reach improvements in performance. High values of BPR for a TIT of 1400 K allow improvements in performance for OPR around 35. The maximum attainable BPR is equal to 7 for FPR=1.7 and equal to 5 for FPR=1.9. At a higher value of TIT equal to 1600 K it is possible to reach even a lower TSFC for a specific thrust of 140 N/kg/s, requiring BPR=10 when FPR= 1.7 and BPR=8 when FPR=1.9. High BPR has a positive effect on TSFC and its optimum value generally leads to a lower specific thrust, but it depends weakly on OPR. For BPR=4.5 a design adopting OPR and TIT around 30 and 1300 K seems to be a reasonable choice for the same power range as requested in the present study. Figure 7 (space of criteria BPR-FPR) permits selecting both BPR and FPR for a balanced design to keep a reasonable specific thrust, and by increasing TIT the propulsive performance improves more. The most advantageous feature retained from the unmixed configuration is the possibility of selecting the specific thrust independently from the gas generator. In addition, FPR is selected freely and BPR controls the size of the bypass and the core as well as the LP turbine stages, thus resulting in a better performance management.

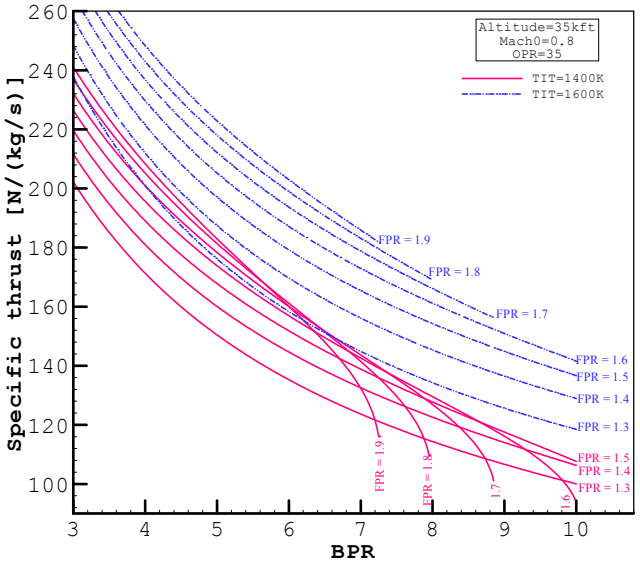

Figure 2: Effect of BPR on specific thrust of unmixed turbofan

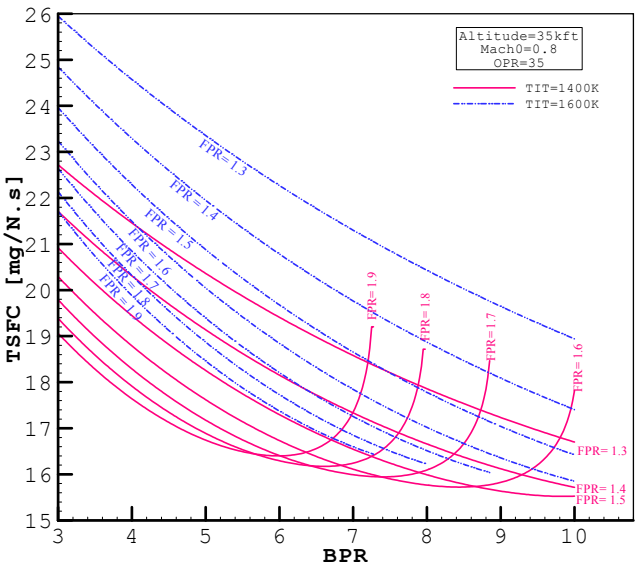

Figure 3: Effect of BPR on TSFC of unmixed turbofan

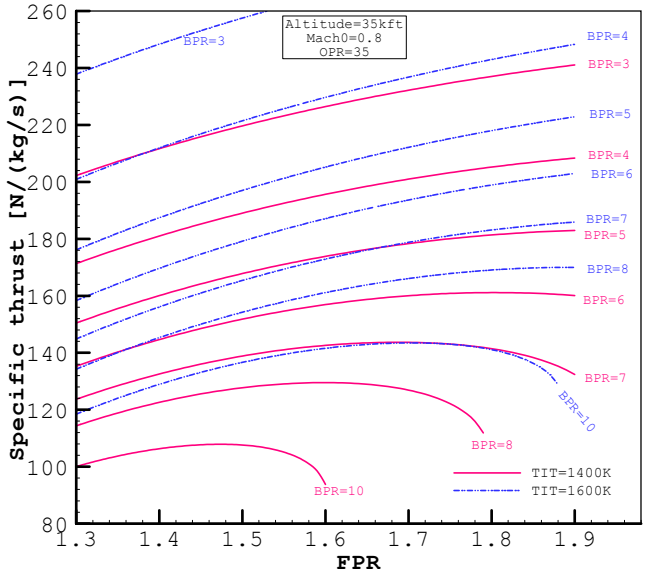

Figure 4: Effect of FPR on specific thrust of unmixed turbofan

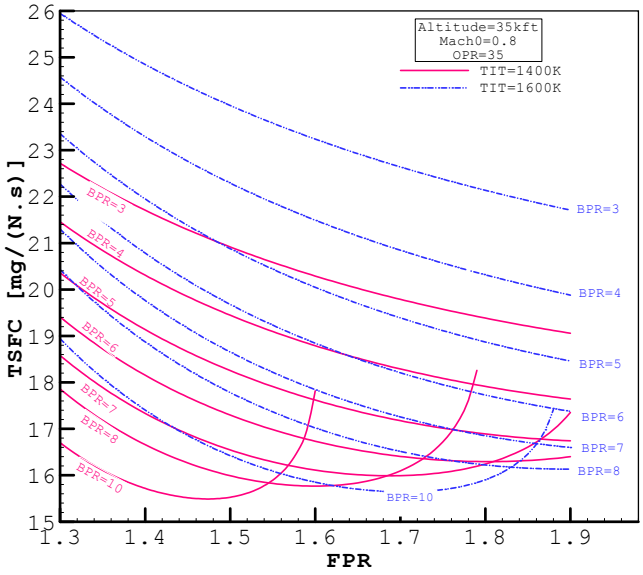

Figure 5: Effect of FPR on TSFC of unmixed turbofan

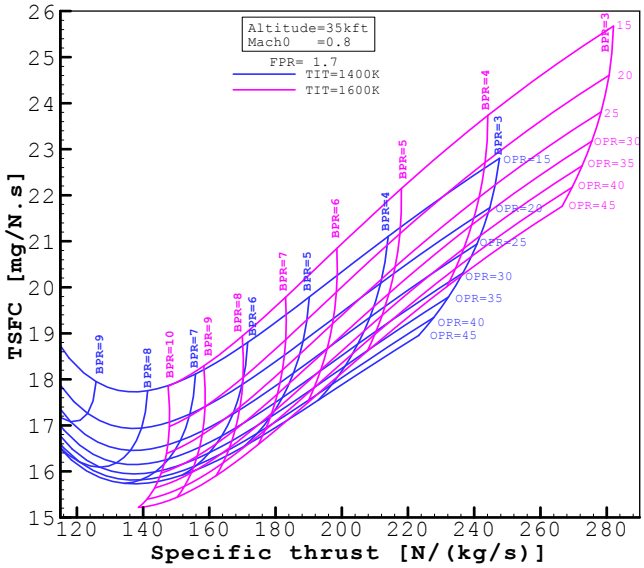

Figure 6: Space of criteria (BPR-OPR) of unmixed turbofan

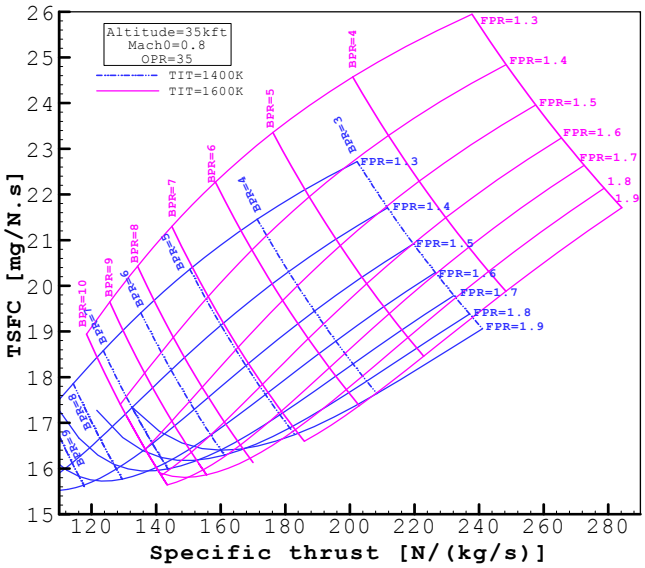

Figure 7: Space of criteria (BPR-FPR) of unmixed turbofan

Parametric Analysis of Mixed Turbofan

Figure 8 illustrates the effects of FPR with BPR, TIT and OPR. The fan provides a sufficient static pressure to the secondary flow, ensuring an efficient mixing between the bypass and core streams. The effects of increasing BPR from 3 to 10 on the specific thrust, for TIT=1400 K and 1600 K, and for OPR=30 and 40, are clearly depicted. The optimum value of FPR (dashed lines) reveals that there is essentially a decrease in the specific thrust with BPR and there is a noticeable increase with TIT. By increasing OPR from 30 to 40 this usually leads to a decrease in the specific thrust. Figure 9 plots the variation of TSFC for two values of TIT and OPR, for the optimum values of FPR (dashed lines). As depicted, high value of BPR has a positive effect on TSFC until an optimum value depending on TIT, but later TSFC increases. The optimum value of BPR evidently depends on OPR and TIT. As seen from Fig. 9 when TIT=1400 K the optimum of BPR is located in between 5 and 6, but for TIT=1600 K it becomes in between 8 and 9. For the optimum of BPR, the convenient value of FPR becomes less for the high values of BPR and OPR, but increases with TIT.

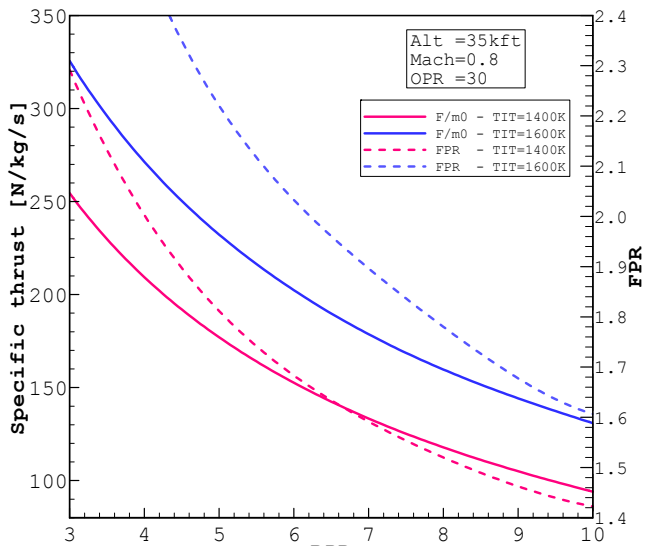

(OPR=30)

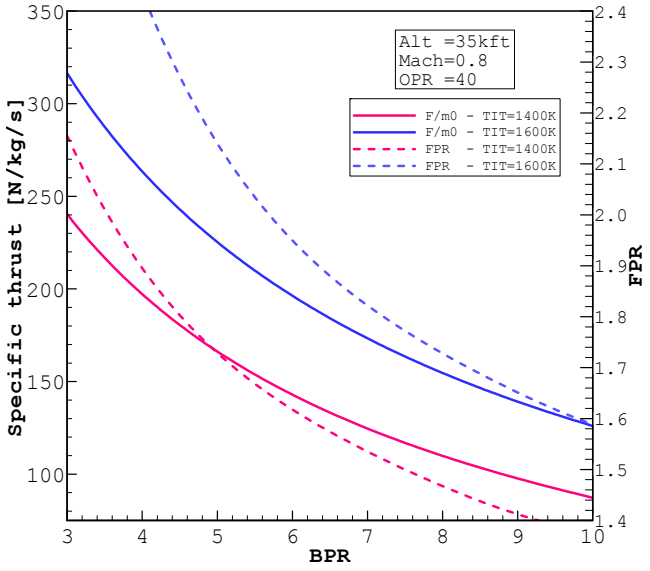

(OPR=40)

Figure 8: Effect of BPR on specific thrust of a mixed turbofan

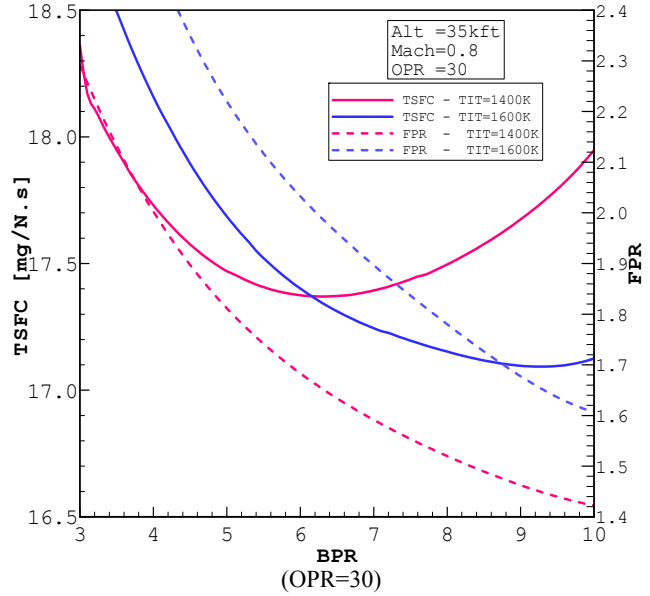

(OPR=30)

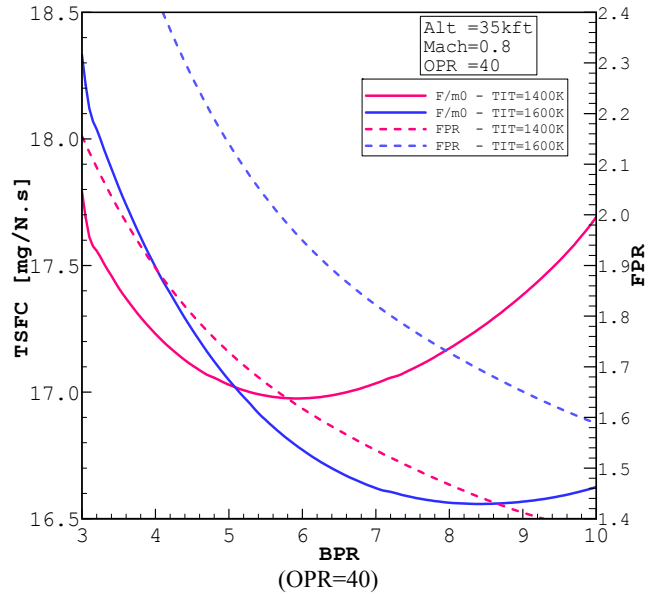

(OPR=40)

Figure 9: Effect of BPR on TSFC of a mixed turbofan

Figure 10 presents the variations of TSFC versus specific thrust (space of criteria TIT-OPR), based on the values of BPR of 5 and 10 and the optimum FPR. The variation of TSFC with TIT depicts a minimum value that drops further more for high values of OPR and BPR. For a given BPR, the optimum of OPR shifts to higher values when TIT is high. According to Fig. 10, the specific thrust tends to increase with TIT but the effect of OPR is less, on the contrary for the low values of TIT. In the other side, OPR has a noticeable effect on TSFC, which continues dropping with it for the high values of TIT. By referring to Fig.10 the effect of BPR is revealed through a drastic decrease in specific thrust from a value of 246.3 N/kg/s to 140.5 N/kg/s, when using BPR=10 instead of BPR=5, for the given OPR=50 and TIT=1700 K. In addition, the effect of BPR on TSFC is noticeable as it drops to a low value of 16.08 mg/Ns for the above values of TIT and OPR. For a high BPR equal to 10, any increase in TIT is beneficial for TSFC, but for the low value of BPR such as 5 there are optimum values of TIT and OPR which beyond the TSFC increases slightly. There are tradeoff values between BPR and TIT keeping TSFC near the minimum and the specific thrust as low as possible. The primary incentive in increasing TIT is improving the specific thrust and hence reducing the engine size, but not at the expense of TSFC which may increase due to the drop in the propulsive efficiency. Figure 11 plots TSFC versus specific thrust (space of criteria BPR-OPR) for TIT=1400 K and 1600 K and the optimum of FPR. The value of BPR generally leads to a low specific thrust; compare between the values of BPR equal to 5 and 10. For a moderate TIT=1400 K, large values of BPR improves the propulsive performance for the high OPR, while the optimum BPR is seen in between 5 and 6. Moreover, high values of TIT=1600 K allow using higher OPR more than 40 combined to the large value of BPR in between 8 and 10. The space of criteria (BPR-OPR) may serve in finding the design parameters based on the iso-contours of TSFC and specific thrust, if the user does not rely on optimization procedure. To decide on the final value of TIT, tradeoffs are required between the maximum thrust at take-off and the technology constraints and emissions.

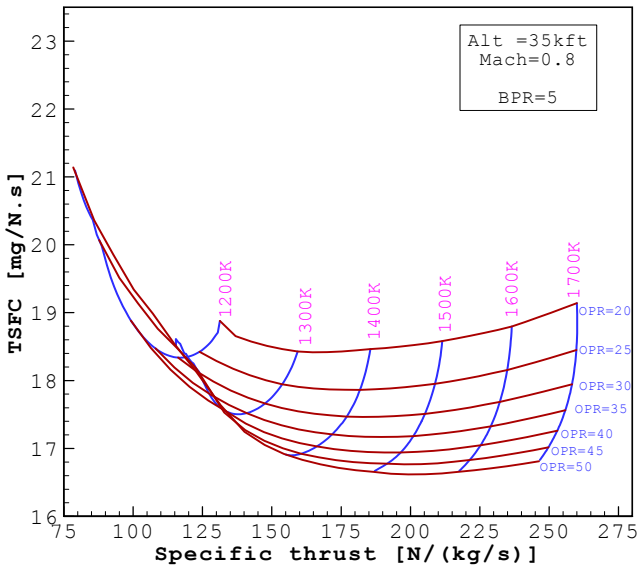

(BPR=5)

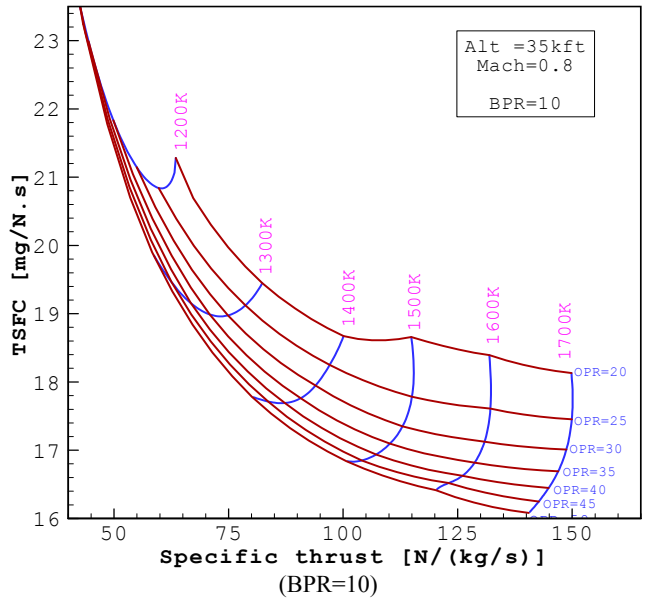

(BPR=10)

Figure 10: Space of criteria (TIT-OPR)

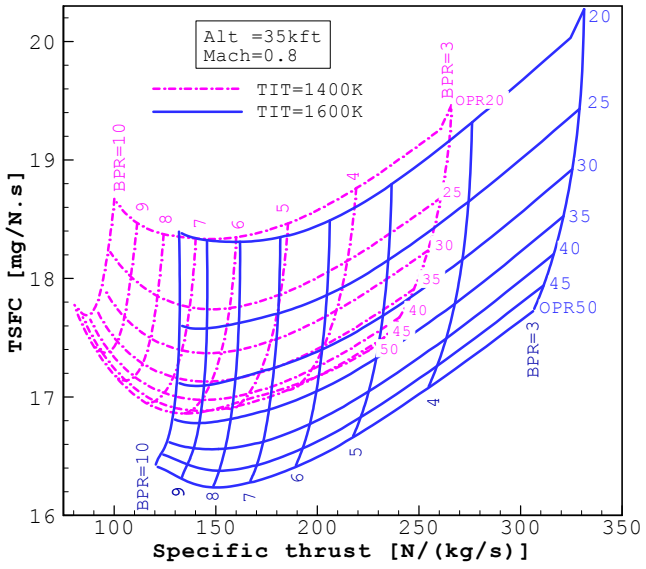

Figure 11: Space of criteria (BPR-OPR)

OFF-DESIGN PERFORMANCE

The determination of off-design performance requires calculating the engine equilibrium and operating lines. These latter assume the availability of the different components' maps and the control schedule, which are necessarily available in the early design. Thus, simpler and direct methods to predict off-design performance are still required. The off-design parameters are estimated via multivariable relationships satisfying the conservations of mass and momentum and energy balance for the HP and LP spools (This methodology is exposed in an early paper by Ghenaiet [20, 21]). The choking conditions of NGVs for HP and LP turbines occur at takeoff (100% maximum rpm) and in cruise at the ratings 95% and 92.5% for LP and HP spools [17]. The introduction of non-dimensional parameters and invariable functions evaluated at the reference point (cruise) led to a non-linear system of equations solved iteratively assuming initial values. The constants k_i, i=1,2…17 are estimated from design point. The throttle ratio relates the turbine inlet total temperatures at different flight conditions.

$$T_{t4} = \frac{\tau_r (T_0/T_{SLS})}{\vartheta_r} T_{t4\max} \tag{9}$$

From the power balance of LP spool, the temperature and pressure ratios of the fan of unmixed turbofan are updated:

$$\tau_F = 1 + \frac{k_1 \tau_b}{1+\alpha/k_2} \frac{1-\tau_{TL}}{\tau_r} \tag{10a}$$

and for the mixed turbofan by:

$$\tau_F = 1 + \left[k_3 (1-\tau_{TL}) \frac{\tau_b \tau_{TH}}{\tau_r} - k_4 \frac{(1+\alpha)}{\tau_r} \right] \Big/ (k_5 + \alpha) \tag{10b}$$

The enthalpy rise of LP compressor comprising the lower part of the fan is proportional to the enthalpy rise, thus the total temperature and pressure ratios of LP compressor are updated by:

$$\tau_{CL} = 1 + k_6 (\tau_F - 1) \tag{11}$$

From the power balance of HP spool, the total temperature and pressure ratios of HP compressor are updated for the unmixed turbofan.

$$\tau_{CH} = 1 + k_7 \frac{T_{t4}}{T_0} \left(\frac{1}{\tau_r \tau_{CL}} \right) \tag{12a}$$

and for the mixed turbofan by:

$$\tau_{CH} = \left[1 + k_8 (1-\tau_{TH})(1+f) \frac{\tau_b}{\tau_r \tau_{CL}} - k_9 \frac{(1+\alpha)}{\tau_r \tau_{CL}} \right] \Big/ k_{10} \tag{12b}$$

The relations between the core and bypass streams when considering a choked HP turbine, yields an equation for the unmixed turbofan BPR updated as follows:

$$\alpha = k_{11} \frac{\Pi_F \sqrt{\tau_b / \tau_r \tau_F}}{\Pi_{CL} \Pi_{CH}} MFP_{19} \tag{13a}$$

Whereas for the mixed turbofan BPR is updated by:

$$\alpha = \frac{k_{12} \pi_F}{\pi_{CL} \pi_{CH} \pi_b \pi_{TH} \pi_{TL}} \sqrt{\frac{\tau_b \tau_{TH} \tau_{TL}}{\tau_r \tau_F}} \frac{MFP_{16}}{MFP_6} \tag{13b}$$

The actual mass flow rate for both configurations is updated:

$$m_0 = k_{13} (1+\alpha)(P_0 \Pi_r \Pi_d \Pi_{CL} \Pi_{CH}) T_{t4}^{-1/2} \tag{14}$$

The expansion parameters are held constant for the choked HP turbine. However, for LP turbine the total pressure and temperature ratios for the unmixed turbofan are updated:

$$\pi_{TL} = k_{14} \sqrt{\tau_{TL}} / MFP_9 \tag{15a}$$

and for the mixed turbofan they are updated iteratively:

$$\tau_{TL} = k_{15} \pi_{TL}^{\ 2} MFP_6^{\ 2} \quad \text{and} \quad \tau_{TL} = 1 - \eta_{sTL} \left[1 - \Pi_{TL}^{(\gamma_{45}-1)/\gamma_{45}} \right] \tag{15b}$$

By considering variations of enthalpy across LP and HP compressors proportional to the square of rotational speeds, the percentage variations of LP and HP speeds of rotation are as follows:

$$\%N_{TL} = k_{16} \sqrt{T_0 \tau_r (\tau_F - 1)} \quad \text{and} \quad \%N_{TH} = k_{17} \sqrt{T_0 \tau_r \tau_{CL} (\tau_{CH} - 1)} \tag{16}$$

The updated values of isentropic efficiencies of fan, LP and HP compressors and LP and HP turbines are based on modified relations due to Flack [22], involving the corrected mass flow rate and rotational speed.

$$\left. \frac{\eta_{is}}{\eta_{is}^*} \right|_c = 1 - k_{18} \frac{N_{co}^*}{N_{isc}^*} \left| 1 - \frac{N_{co}}{N_{co}^*} \right| - k_{19} \frac{\dot{m}_{co}^{*2}}{\eta_{isc}^* N_{co}^*} \left[1 - \frac{\dot{m}_{co}}{\dot{m}_{co}^*} \right]^2 \frac{N_{co}^*}{N_{co}} \tag{17a}$$

$$\left. \frac{\eta_{is}}{\eta_{is}^*} \right|_t = 1 - k_{20} \left[\frac{1 - \pi_t^{ch}/\pi_t}{1 - \pi_t^{ch}} \right]^2 - k_{21} \left[1 - \frac{\dot{m}_{co}}{\dot{m}_{co}^{ch}} \frac{N_{co}}{N_{co}^*} \right]^2 \tag{17b}$$

All the updated parameters are re-iterated until the total convergence.

OPTIMIZATION

The parametric analysis does not necessarily lead to the proper optimum, but can produce useful information over the ranges of specified design parameters. With many involved variables and constraints only optimization procedure can lead reasonably to the optimum. For a transport aircraft there are different possible design points, however the cruise flight (excellent specific fuel consumption) seems the most distinguishable and engines are optimized around this goal [23]. The thrust at takeoff to reach an altitude of safety must be satisfied and the pollutants are a matter of concern. Extreme operating conditions, such as takeoff, are assessed by off-design computations referring to the flight performance analyses, such as reported by Ghenaiet [14]. The physical limitations (constraints) of the design variables are listed in Table 3 and the engine requirements in Table 4. High values of BPR around 10 are considered by designers, but entail a growth in engines diameters and sensitivity to flight conditions. The intake throat diameter is related to the maximum corrected mass flow rate of air and generally determined [24] as follows:

$$d_{th} = \sqrt{1.273 \frac{\sqrt{T_{sls}}\left[\dot{m}_{0_{CO}}\right]_{max}}{P_{sls}\, MFP(M_{th}=0.8)}} \tag{18}$$

High value of TIT is thermodynamically desirable but needs complex cooling of HP turbine blades, On the other hand, for uncooled LP turbine, the inlet temperature should not exceed a certain limit. For high bypass turbofans, high values of OPR and subsequently HPR are recommended for further improving TSFC, hence the exit temperature of HP compressor stages should be limited. Value of FPR from 1.4 to 1.8 allows in an unquestionable manner more energy to the bypass airflow that is more constrained in the case of mixed turbofan. Moreover, the matching of the turbines stages with the compression stages necessitates limiting their expansion ratios in between 0.85 - 0.89 by a turbine stage [16].

The constraints of pollutants NOx, CO, UHC estimated based in terms of mass of emittant per unit of maximum engine thrust as a function of emission index 'EI' defined as grams of emission per kilogram of fuel consumed and time of operation.

$$DP/thrust = \sum_{i=1}^{4} time_i . \dot{m}_{f_i} . EI_i \Big/ F_{TO} \tag{19}$$

Emission index for NOx is based the General Electric correlation [25], whereas for CO and UHC are due to Wulff and Hourmouziadis [26]. The summation denotes the fact that an aircraft operates at different power settings: take-off, climb, approach and idle. The emissions limits are specified according to ICAO [27].

The design optimization problem is stated as: minimize TSFC in cruise flight condition (Mach=0.8, altitude=35kft, standard day) for the given thrust level, while respecting the thrust at take-off (hot day) greater than the requirement, according to the constraint diagram [14]. Cruise fuel consumption of turbofan engines is a key metric for increasing airline profitability and reducing CO_2 emissions. By considering a throttle ratio equal to unity, there are six design parameters to be optimized in the same time: air mass flow rate, BPR, FPR, LPR, HPR and TIT. This problem of optimization is formulated as follows:

$$\begin{cases} \text{Maximize}\,(1/\text{TSFC}) \\ \text{under}: g_i\left(\vec{X}\right) \le 0 \qquad i = 1,2,....n_c \\ \qquad x_{kL} \le x_k \le x_{kU} \quad k = 1,2,....n_v \end{cases} \tag{20}$$

The following optimization cases are considered:

- Case 1: three constraints
- Case 2: seven constraints
- Case 3: ten constraints (including pollutants emission)

To carry out optimization there are essentially four developed programs modules written in Fortran, in addition to other subroutines: The master program and the on-design and off-design analyzers as well as the optimizer GA algorithm "PIKAIA" [28]. The determined search space was crucial so that the optimization converged rapidly towards the physical stable solutions, while respecting all the requirements and constraints. The good conditioning for the space of criteria obtained from the preliminary parametric study led to Table 3 showing the intervals of different variables and the Table 4 summarizing imposed constraints.

A penalty function was incorporated, and since the constraints are normalized and violations take more or less the same order of magnitude, they are simply summed. Deb [29] has stipulated that if the solution is infeasible (at least one constraint is violated) the designer will penalize the objective function. Mathematically the fitness function is written in the following form:

$$F(\mathrm{X}) = \begin{cases} f(\mathrm{X}) & \text{if } g_j(\mathrm{X}) \ge 0 \\ f_{max} + \sum_{j=1}^{Nc} \left| g_j(\mathrm{X}) \right| & \text{otherwise} \end{cases} \tag{21}$$

Table 3: Range of design parameters

Parameters	minimum	maximum
BPR	3	10
FPR for unmixed turbofan	1.4	1.9
HPR	7	15
LPR	2	6
TIT(K)	1250	1600
Air mass flow rate (kg/s)	200	400

Table 4: Constraints

	Constraints		Type	limits
1	Thrust at cruise		≥	52 kN
2	Thrust at take-off		≥	277 kN
3	TIT at take-off		<	1600 K
4	Entry temperature to LP turbine		<	1250 K
5	Exit temperature from HP compressor		<	850 K
6	Temperature expansion ratio:			
		HP turbine	≥ ≤	0.7 - 0.79
		LP turbine	≥ ≤	0.6 - 0.7
7	Pollutants:			
		$[Dp/F_{TO}]_{CO}$	≤	118 (g/kN)
		$[Dp/F_{TO}]_{UHC}$	≤	19.6 (g/kN)
		$[Dp/F_{TO}]_{NOX}$	≤	depends on OPR

RESULTS

The parametric study constituted the necessary data to delimit the search space and to locate the active constraints for optimizing the design parameters of unmixed and mixed

high bypass turbofan engines. As results, the found optimum parameters are air mass flow rate, TIT, BPR, FPR and OPR (LPR, HPR), concurrently minimizing TSFC for the requested level of thrust in cruise and takeoff while meeting the active constraints. The optimization process required some data related to the engine match point defined by the thrust by weight ratio and aircraft wing loading [14]. The results of optimization are presented in Table 5 and Table 6 for the unmixed and mixed turbofan engines. For the unmixed turbofan, by considering all the constraints (case 3) BPR is found equal to 4.85 due to pollutants limits but is equal to 4.077 for case 2 that included temperature and expansion limitations, whereas for the less constrained case 1 (only three constraints) BPR is equal to 4.56. The optimum of BPR involved trade-offs between flight performance requirements and the limitations imposed on the components and intake. The resulting intake throat diameter is equal to 2.278 m for the most constrained case 3, which compare to engines of same power range. For the allowable material temperature of turbine blade equal to 1600 K the optimum TIT in cruise is equal to 1371.2 K which is practically the same between the three cases. At takeoff, TIT is equal to 1599.4 K which is practically the same for the three cases. This permissible TIT is good for the sustainability of nowadays engines. For the most constrained case 3, the entry temperature to LP turbine has a value of 1174.3 K. The constraints of expansion ratios of HP and LP turbines reach values of 0.669 and 0.62 (case 1), whereas these values are 0.705-0.725 and 0.726-0.712 for the case 2 and 3, thus allowing using two or three HP turbine stages and four or five LP turbine stages. The optimum value of OPR reaches a value of 53.42 when there are only three constraints (case1), but is equal to 32.38 for case 2 and has a lesser value of 26.88 for the case 3 (with all constraints). Indeed, this lowest value of OPR in the case 3 is imposed by the NOx emission limitation. The optimum FPR in case 1 is equal to 1.758, and equal to 1.799 and 1.787 in the case 2 and 3, which seems following the variation of BPR that affected the expansion of LP turbine. This adequate value of FPR allows giving more energy to the bypass stream and subsequently the secondary thrust. The booster (LPR) reaches a value 4.39 for the less constrained case 1, but is equal to 2.29 and 2 for the constrained case 2 and 3. The high value of LPR in the case 1 tends to compensate for the relatively low HPR. This boosting compressor requires 2 or 3 stages including the lower part of the fan as it rotates at a lower speed. For a stable operation in addition to the allowable operating temperature of compressor blades, there is a limitation for the maximum OPR. Indeed, the exit temperature of HP compressor does not exceed 850 K for the constrained case 2 and is even lower for the case 3 reaching a value of 802.56 K. The design mass flow rate in cruise is around a value of 368 kg/s for the most constrained design case 3, whereas at takeoff is equal to 838 kg/s which in fact close to the mass flow rates of turbofans of similar power range, i.e. CF6-80C2 engine. For the allowable temperature of 1600 K, the case 3 offers a larger thrust potential of 66883.42 N more than required. The TSFC in cruise reaches the values of 16.34 mg/Ns, 17.83 mg/Ns and 17.61 mg/Ns for the cases 1, 2 and 3, respectively, whereas at take-off TSFC has the values of 9.59 mg/Ns, 11.04 mg/Ns and 10.72 mg/Ns, for cases 1, 2 and 3 respectively. Obviously, the case 1 leads to lesser TSFC since there are only the constraints of thrust in addition to TIT limit, whereas in the case 2 the constraints of temperatures and turbines expansion ratios constrained the work transferred. The target design case 3 led to slightly less fuel consumption than case 2 owing to the effect of emissions constraints. The case 3 produces a specific thrust of 181.69 N/kg/s whereas in the case 1 it is equal to 162.07 N/kg/s, mainly due to more mass flow rate. The NOx pollutant is shown to reduce from 196.36 g/kN to 66.99 g/kN between the design cases 1 and 3. Indeed, the key parameters in controlling this emission are the pressure and the combustor temperature. On the contrary, the other pollutants such as CO and UHC tend to increase when reducing OPR but without exceeding the limits. For the target design case 3 the emissions levels of 117.98 g/kN and 13.93 g/kN are found for the pollutants CO and UHC, respectively. Finally, this design of unmixed high bypass engine, reaching practically for the same TSFC as the reference engine, seems to produce higher thrust potential at both takeoff and cruise for a lesser overall pressure ratio. For this category of high bypass turbofan in the same power range, the prescribed design will adopt similar parameters around BPR=4.5, OPR=27 and FPR=1.75, in addition to TIT=1370 K for a better sustainability of turbines blades.

Table 5: Optimized high bypass unmixed turbofan engine

Unmixed turbofan	Case 1	Case 2	Case 3
Air mass flow rate (kg/s)	399.960	349.500	368.106
BPR	4.5623	4.0779	4.8460
FPR	1.7585	1.7999	1.7870
LPR	4.3884	2.2898	2.0351
HPR	12.1728	14.1419	13.2104
OPR	53.4201	32.3830	26.8850
TIT (K)	1371.53	1367.68	1371.21
Performance in cruise (altitude =10668m & Mach=0.8, ISA)			
Thrust (kN)	64821.48	68047.16	66883.42
TSFC (mg/N.s)	16.3439	17.8318	17.6166
Specific thrust (N/kg/s)	162.069	194.698	181.696
Intake diameter (m)	2.3753	2.2204	2.2788
Constraints at takeoff			
Air mass flow rate (kg/s)	908.745	795.266	838.004
TIT (K)	1599.83	1595.34	1599.46
T_{t3} (K)	986.79	849.70	802.56
T_{t45} (K)	1085.86	1139.54	1174.28
τ_{TH} HP expansion ratio	0.6691	0.7054	0.7258
τ_{TL} LP expansion ratio	0.6201	0.7261	0.7123
Performance at takeoff (altitude =0m & hot day)			
Thrust (kN)	277359.8	277400.6	277311.6
TSFC (mg/N.s)	9.5944	11.0384	10.7237
Specific thrust (N/kg/s)	305.212	348.814	330.919
Air mass flow rate (kg/s)	908.745	795.266	838.004
Intake diameter (m)	2.3753	2.2204	2.2788
Pollutants emissions			
$[Dp/F_{TO}]_{CO}$ (g/kN)	58.834	95.344	117.979
$[Dp/F_{TO}]_{UHC}$ (g/kN)	0.746	4.476	13.936
$[Dp/F_{TO}]_{NOX}$ (g/kN)	196.360	93.240	66.994

For the mixed turbofan engine, the optimization was carried out considering similar search space. For the mixed turbofan, by considering all the constraints (case 3) BPR is

found equal to 4.252 due to pollutants limits, and equal to 3.398 when the limits of temperatures and expansion ratios are active, whereas for the lesser constrained case 1 BPR becomes equal to 4.662. The resulting intake throat diameter for the constrained case 3 is equal to 2.266 m, whereas for case 1 this diameter is even lower and equal to 2.183 m. For the allowable turbine temperature of 1600 K, the optimum value of TIT in cruise has the lowest value of 1301.89 K but at takeoff it is equal to 1518.6 K which is good for the engine lifetime. The entry temperature to the LP turbine has a value of 1124.41 K for the constrained case 3. The constraints of expansion ratios of HP and LP turbines are at values of 0.6437 - 0.6659 for case 1, 0.7144 - 0.6517 for case 2 and 0.7420 - 0.7098 for case 3, thus adopting two or three stages for HP turbine and four or five stages for LP turbine. The optimum OPR has a value of 44.25 for the case 1, but becomes equal to 32.08 and 21.42 for case 2 and case 3, respectively. The OPR in the case 3 is even lower than that of unmixed turbofan. In order to satisfy the coupling between the core and secondary flows, as there is a constraint of static pressures equality at the mixing plane between the bypass airflow and the core flow, an ideal value of FPR has to be evaluated within the optimization loop. Thus, in case 1 FPR is equal to 1.559, but becomes higher and equal to 1.8576 and 1.8182 for the cases 2 and 3, respectively. This tendency seems to follow the variation of BPR, which affects the LP turbine expansion and subsequently the mixing conditions. The boosting compressor (LPR) reaches a value of 3.8529 for the less constrained case 1 and is higher and equal to 4.7867 for case 2 to compensate for the drop in HPR. The lowest value of LPR obtained for case 3 could be attributed to the drop in OPR imposed by NOx emission and the moderate value of core pressure related to mixing condition. The exit temperature of HP compressor does not exceed 896.93 K for case 2 and even lower for the case 3 reaching a value of 760.21 K. The obtained design mass flow rate in cruise for the most constrained design case 3 is around 364 kg/s and equal to 953.3 kg/s at takeoff, which is higher than that found for the unmixed turbofan. For the maximum allowable temperature of 1600 K, the design of case 1 offers higher thrust because of highest core pressure and temperature, whereas the most constrained case 3 still offer a sufficient thrust potential of 60467.82 N. In cruise TSFC reaches the values of 14.30 mg/N.s, 17.27 mg/N.s and 19.44 mg/N.s for the cases 1, 2 and 3, respectively, and at take-off these values are 8.72 mg/N.s, 10.29 mg/N.s and 11.14 mg/N.s, respectively. As noticed the case 1 leads to lesser TSFC because there are only the constraints of thrust in addition to TIT limit. The target design case 3 led to higher TSFC than the case 1 due to low core pressure and subsequently the drop in thermal efficiency. However, the hourly fuel consumption is practically the same in both cases. The specific thrust in case 3 is equal to 166.12 N/kg/s, which is equal to 171.15 N/kg/s in case 1, as related to the drop in the cruise thrust and air mass flow rate. The NOx pollutant is shown to diminish from 191.01 g/kN to 60.43 for the design cases 1 and 3, since the OPR reduced significantly. In the other side, the pollutants such as CO and UHC tend to increase by reducing OPR. For the target design case 3 the pollutants CO and UHC are far below the limits and reach values of 92.20 g/kN and 1.21 g/kN, respectively. As noticed, these levels of pollutants are lesser than obtained for the unmixed turbofan. This design of mixed high bypass engine leads to a slightly higher TSFC, but requires low OPR and hence lesser weight for practically the same intake diameter of unmixed turbofan. For the same power range of 280 kN a design adopting the parameters of BPR=4.25, OPR=22 and FPR=1.8 in addition to TIT=1300 K seems to be undoubtedly a judicious choice since less expensive materials have to be used.

Table 6: Optimized high bypass mixed turbofan engine

Mixed turbofan	Case 1	Case 2	Case 3
Parameters in cruise			
Air mass flow rate (kg/s)	391.686	338.032	364.000
TIT (K)	1371.28	1327.13	1301.89
BPR	4.6620	3.3983	4.2518
FPR	1.5590	1.8576	1.8182
LPR	3.8529	4.7867	2.1701
HPR	14.4020	8.2797	9.8735
OPR	55.4900	39.6329	21.4265
Performance in cruise (altitude =10668m - Mach=0.8, ISA)			
Thrust (kN)	67039.77	64849.98	60467.82
TSFC (mg/N.s)	14.3075	17.2690	19.4439
Specific thrust (N/kg/s)	171.1569	191.8457	166.1204
Intake diameter (m)	2.3506	2.1837	2.2660
Constraints at takeoff			
TIT (K)	1599.54	1548.04	1518.60
T_{t3} (K)	981.17	896.93	760.21
T_{t45} (K)	1050.50	1113.73	1124.41
τ_{TH} HP expansion ratio	0.6437	0.7144	0.7420
τ_{TL} LP expansion ratio	0.6659	0.6517	0.7098
Performance at takeoff (altitude =0m & hot day)			
Thrust (kN)	279578.2	277584.2	277619.9
TSFC (mg/N.s)	8.7298	10.2985	11.1490
Specific thrust (N/kg/s)	268.6021	317.9422	291.1986
Air mass flow rate (kg/s)	1040.864	873.065	953.369
Intake diameter (m)	2.3506	2.1837	2.2660
Pollutants emissions			
$[Dp/F_{TO}]_{CO}$ (g/kN)	59.197	69.425	92.205
$[Dp/F_{TO}]_{UHC}$ (g/kN)	0.685	0.828	1.211
$[Dp/F_{TO}]_{NOX}$ (g/kN)	191.016	124.788	60.432

The uninstalled performance of the two configurations of high-bypass turbofan were evaluated at different flight conditions based on the optimized case 3, for TIT limits (1600 K) and a throttle ratio equal to 1. The bypass ratio increases with Mach number but drops with the altitude (not shown here) due to reduced swallowing capacity of the bypass duct, hence diverting the extra air mass flow to the core. The air mass flow rate increases with the flight velocity and decreases with the altitude due to lesser air density. Above certain limits imposed by the control schedule, the values of FPR, LPR and HPR (not shown here) drop with Mach number but increase with the altitude. The thrust at different flight conditions are plotted in Fig 12 and Fig 13. The thrust is shown to decrease with velocity mainly via increased free stream momentum, which is clearer at the sea level. At high altitudes from 20 - 35 kft, the thrust tends to stabilize owing to reduced intake momentum. The TSFC tends to increase with the flight speed, but on the contrary,

decreases with altitudes especially near the ceiling level. The mixed turbofan seems to offer a better acceleration potential at higher cruising speed and good fuel consumption. The integration and installation penalty of such engines will give the final assessment of the two configurations.

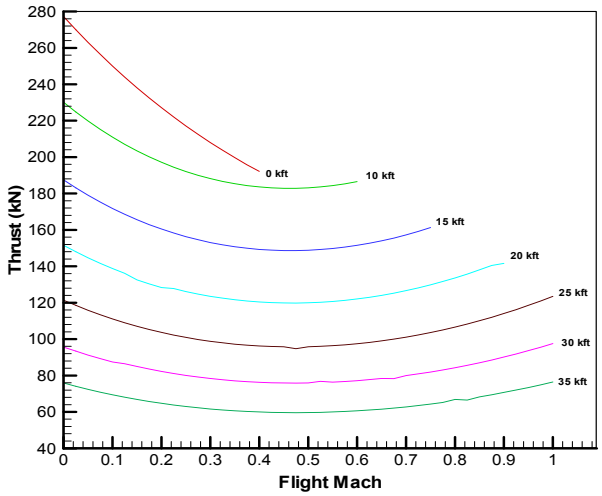

(a)

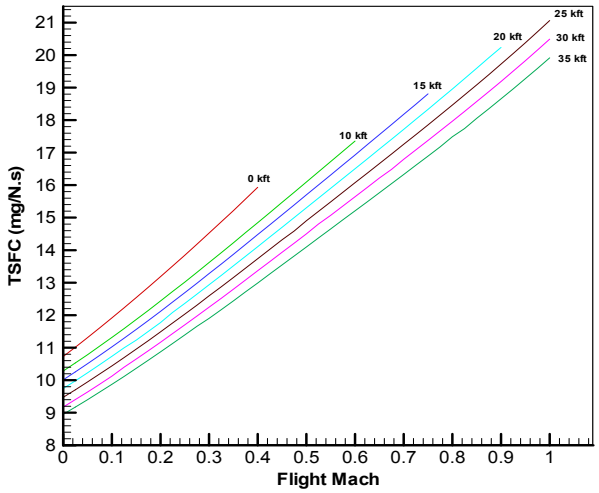

(b)

Figure 12: Performance of optimized high-bypass unmixed turbofan: case 3 of TIT_{limit}=1600 K: a) Thrust, b) TSFC

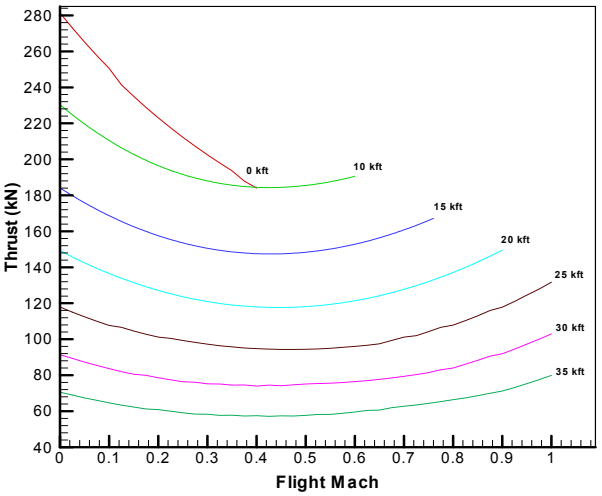

(a)

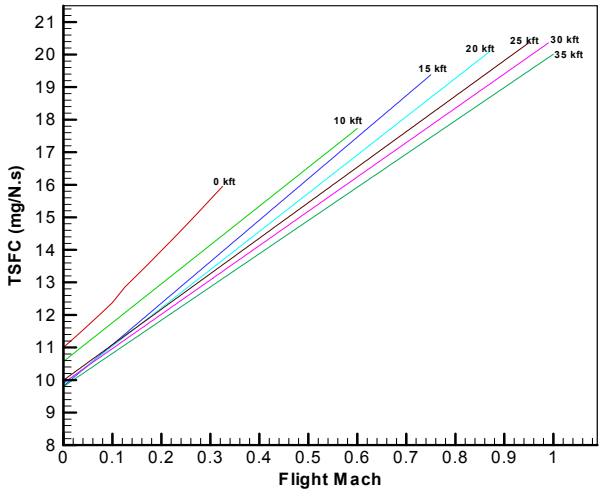

(b)

Figure 13: Performance of optimized high-bypass mixed turbofan: case 3 of TIT_{limit}=1600 K: a) Thrust, b) TSFC

CONCLUSION

The preliminary design of unmixed and mixed turbofan engines in the power range of 280 kN has dictated utilizing a high BPR and a moderate TIT for a better durability. The increase in BPR is a natural choice for this category of aero-engines as it improves TSFC, but entails higher intake diameter and offsets the flow path between the fan and the core as well as a high number of LP turbine stages. In the configuration of mixed turbofan, FPR strongly depends on the mixing conditions. Utilization of a common propelling nozzle leads to improving the core cooling, and better propulsive efficiency attributed to higher mixed temperature upstream of the common nozzle, as well as less emissions of mixed gases. The preference for mixed exhaust turbofan installations in some commercial airliners is primarily because of improvements in thrust and TSFC. New models for the components efficiencies and the updated database of foreseeable engines technology are required, in addition to adopting more robust hybrid optimization algorithms.

NOMENCLATURE

A	Area [m^2]
C_{to}	Coefficient of power extraction
cp	Specific heat [J/kg.K]
d	Diameter [m]
e	Polytropic efficiency
f	Fuel by air ratio
F	Thrust [N]
k_1 - k_{17}	Constants in off-design analysis
Lcv	Lower calorific value of fuel [J/kg]
$\dot{m}$	Mass flow rate [kg/s]
M	Mach number
MFP	Mass flow rate parameter
N	Rotations per minutes [rpm]
P	Pressure [Pa]
R	Gas constant [J/kg.K]
T	Temperature [K]
V	Velocity [m/s]

Greek symbols

α	Bypass ratio
β	Air bleed fraction
ε	Air cooling fraction

γ	Isentropic index
η	Efficiency
Π	Pressure ratio
τ	Total temperature ratio

Subscripts

b	Burner
c	Compressor
ch	Choked
co	Corrected mass flow or rotational speed
d	Diffuser
F	Fan
g	Gas mixture
H	High pressure
is	Isentropic
L	Low pressure
m	Mechanical
mx	Mixer
n	Nozzle, normal
r	Ram compression
T,t	Turbine, total
th	Throat
TO	Take-off
*	Design point
0	Upstream of intake
1 - 9	Station numbering

Abbreviations

BPR	Bypass ratio
FPR	Fan pressure ratio
LPR	Low pressure ratio
HPR	High pressure ratio
ICAO	International Civil Aviation Authority
OPR	Overall pressure ratio
F/m_0	Specific thrust [N/kg/s]
TIT	Turbine inlet temperature [K]
TSFC	Thrust specific fuel consumption [mg/N.s] - [kg/N.h]
ISA	International standard atmosphere
sls	Sea level static conditions

REFERENCES

[1] Ruffles, P.C., 2000, "The future of aircraft propulsion", IMechE, Part C, *Journal of Mechanical Engineering Science*, 2000, 214, (C1), pp 289-305

[2]Birch, N.T., 2000, "The prospects for large civil aircraft propulsion", *Aeronautical J*, August 2000, 104, (1038), pp 347-352

[3] Horobin, M., 1999, "Cycle-match models used in functional engine design - an overview, Design principles and methods for aircraft gas turbine engines", RTO-MP-8, February 1999

[4] Kurzke, J., 1995, "Advanced user-friendly gas turbine performance calculations on a personal computer", ASME paper 95-GT-147,

[5] Visser, W. P. J., and M. J. Broomhead, 2000, "GSP, A generic object-oriented gas turbine simulation environment", ASME Paper 2000-GT-0002, May 2000.

[6] Lytle, J.K. 2001, "The Numerical propulsion system simulation: an advanced simulation tool for airbreathing engines", ISABE 2001-1216

[7] Kurzke, J. 1999, "Gas turbine cycle design methodology: A comparison of parameter variation with numerical optimization", *ASME Journal of Engineering for Gas Turbine and Power*, Vol. 121, January 1999, pp. 6-11.

[8] Sanghi, V., Lakshmanan, B. K. and Sane, S.K., 2001, "Optimum mixing of core and bypass streams in a high bypass civil turbofan", AIAA 2001-3618, 2001

[9] Sane S.K., Tagade, P., and Sanghi, V., 2004, "Optimum propulsion system selection for long range civil transport aircraft", AIAA 2004-3314, 40th AIAA/ASME/SAE/ASEE, Joint Propulsion Conference and Exhibit, 11-14 July 2004, Florida

[10] Jorge de Luis and Mavris D.N., 2004, "Prediction methodology of an optimum turbofan engine cycle", 10th AIAA/ISSMO Multidisciplinary Analysis and Optimization Conference 30 August - 1 September 2004, Albany, New York, AIAA 2004-4363

[11] Yadav, R., Kapadi, Y. and Pashilkar, A., 2005, "Aero-thermodynamic model for digital simulation of turbofan engine", Paper No. GT2005-68248, pp. 63-70; 8 pages

[12] Rybakov, V.N., Kuz'michev, V.S., Tkachenko A.Y and Krupenich I.N., 2016, "Thermodynamic multi-criteria optimization of the unified engine core for the line of turbofan engines", Paper No. GT2016-57854

[13] Syed Khalid, 2016, "Aerothermodynamic benefits of mixed exhaust turbofans", 52nd AIAA/SAE/ASEE Joint Propulsion Conference, July 25-27, 2016, Salt Lake City, UT AIAA 2016-4641

[14] Ghenaiet, A., 2007, "Determination of minimum thrust requirement for a passenger aircraft", *AIAA Journal of Aircraft*, Vol. 44, No. 6, November–December 2007

[15] Davis. D.Y. and Stearns, E.M., 1985, "Energy efficient engine, flight propulsion system final design and analysis". General Electric Company, NASA-Lewis Research Center, Contract NAS3-20643, August 1985

[16] Mattingly, J.D., 1996, *"Element of gas turbine propulsion*", McGraw-Hill international edition 1996

[17] CF6-80 A3, Notebook, General Electric Company, Mail Drop G-2, Aircraft Engine Business Group, Cincinnati, Ohio 45215-6301, Edition 6 – IM , June 1, 1983

[18] Walsh, P.P. and Fletcher, P., "*Gas turbine performance*", 2nd ed., Blackwell Publishing, Fairfield, NJ, pp. 227 and 282.

[19] Pratt&Whitney Aircraft Group JT8D-17A Turbofan engine, SPEC. No. 6281, Date 6-27-80

[20] Ghenaiet, A., 2000, "An approximation method for jet engines flight performances prediction", ASME paper 2000-GT-0149

[20] Ghenaiet, A., 2000, "An approximation method for jet engines flight performances prediction", ASME paper 2000-GT-0149

[21] Ghenaiet A**,** 2008, "Analyses and optimization of a propulsion cycle for unmixed high bypass turbofan", ASME paper GT2008-50340, Proceedings of ASME Turbo Expo 2008, June 9–13, 2008, Berlin, Germany

[22] Flack, R.D., "Analysis and matching of gas turbine components", International Journal of Turbo and Jet Engines, 7, 217-226, 1990

[23] Stevenson, J.D, Saravanamutto, H.I.H., 1995, "Simulating indirect thrust measurement methods for high-bypass turbofans", *ASME J. of Engineering for gas turbine and power*, January 1995, Vol. 117/ pp38-46

[24]Goldsmith, E.L. and Seddon, J., "*Practical intake aerodynamic design*", AIAA Education Series, 1993

[25] Tsalavoutas, A., Kelaidis, M. Thoma, N. and Mathioudakis, K., 2007, "Correlations adaptation for optimal emissions prediction", ASME paper GT2007-27060

[26] Wulff, A., Hourmouziadis, J., 1999, "A universal combustor model for the prediction of aeroengine pollutant emissions", ISABE 99-7162

[27] International Civil Aviation Organization, 1993, "Aircraft engine emissions", Annex 16, Volume II, ICAO, Montreal, 1993

[28] http://www.hao.ucar.edu/Public/models/Pikaia/Pikaia.html

[29] Deb, K., 2000, "An efficient constraint handling method for GA", CMAME 2000